Desalination and Water Treatment
www.deswater.com
doi: 10.1080/19443994.2014.952669

56 (2015) 1809–1819
November

Taylor & Francis
Taylor & Francis Group

Design of multi-N-functional magnetic PVA microspheres for the rapid removal of heavy metal ions with different valence

Xue Bai[a,b,*], Bei Yang[a], Haixin Gu[a], Zulin Hua[a,*], Lu Yu[a], Hanchang Shi[b]

[a]*Key Laboratory of Integrated Regulation and Resource Development on Shallow Lake of Ministry of Education, College of Environment, Hohai University, Nanjing 210098, P.R. China, Tel. +86 15951940543; email: baixue@hhu.edu.cn (X. Bai), Tel. +86 18751958676; email: yangbeimail@126.com (B. Yang), Tel. +86 15252481518; email: ghxhhu@gmail.com (H. Gu), Tel. +86 13505172652; email: zulinhua@hhu.edu.cn (Z. Hua), Tel. +86 15195876772; email: sun.shine.hi@163.com (L. Yu)*
[b]*State Key Joint Laboratory of Environmental Simulation and Pollution Control, School of Environment, Tsinghua University, Beijing 100084, P.R. China, Tel. +86 01062773095; email: hanchang@tsinghua.edu.cn (H. Shi)*

Received 6 January 2014; Accepted 31 July 2014

ABSTRACT

In this study, magnetic polyvinyl acetate (MPVA) microspheres were prepared with the inverse suspension cross-linked method by adding magnetic nanoparticles (Fe_3O_4) into the PVA gel. Then, the resulting MPVA microspheres were modified with amino and ethylenediamine tetra acetic acid (EDTA) groups, which are both associated with nitrogen chelation. The final product, multi-N-functional MPVA (N-MPVA) microspheres, was characterized by scanning electron microscopy, infrared spectroscopy, X-ray photoelectron spectroscopy, and vibrating sample magnetometer. Characterization results showed that the diameter of N-MPVA was about 10 μm; its saturation magnetization value was 4.89 emu g^{-1}, and it possessed abundant amino and EDTA groups. A series of adsorption experiments were conducted to investigate the adsorption behavior, adsorption kinetics, and isotherms of different mono-, di-, and tri-valent heavy metals, i.e. Ag^+, Cu^{2+}, and Cr^{3+}. Results showed that the adsorption capacity of heavy metals with different valences was $Ag^+ > Cu^{2+} > Cr^{3+}$. After three recycles, the loss of adsorption capacity did not exceed 25%. In addition, the chelating mechanism of the amino and EDTA groups with different valences was studied. This present work introduces the potential for using N-MPVA as an effective and recyclable adsorbent for the removal of heavy metal ions.

Keywords: PVA; Magnetism; Functional; Adsorption; Chelating mechanism

1. Introduction

Heavy metal contamination in aqueous solutions originate from many sources, such as metal plating facilities, mining operations, pigment manufacturing, petroleum refining, and tanneries [1]. Many heavy metals in small amounts are important to the regular process of biological cycles. However, when these metals exceed a certain concentration, they may result in various diseases and disorders through bioaccumulation in the food chain [2]. For example, silver may induce the de-energization of cells and disrupt DNA replication [3]; copper may damage cell membranes and cause plant cell death [4]; chromium is an essential trace element for health, but it also causes some

*Corresponding authors.

diseases when its dosage oversteps the normal range [5]. Over the past decade, various methods, such as chemical precipitation, flotation, oxidation reduction, and biological methods, have been used to remove heavy metals [6]. However, every method has its own shortcomings in terms of complexity, efficiency, reusability, and cost. Considered as an effective approach to remove toxic heavy metals from wastewater, adsorption has attracted considerable attention [7,8]. Two types of methods are always used to further enhance the adsorption ability of absorbent: expansion of the specific surface area of an absorbent and modification of different functional groups onto an absorbent.

Increasing the porosity of adsorption materials can increase specific surface areas, such as by applying porous NaY or activated carbon [9–11]. Decreasing the volume of adsorption materials can also achieve the same effect. PVA microspheres prepared through inverse suspension cross-linked method are stable and non-toxic. Importantly, they have large specific surface areas [12]. However, the PVA microspheres are difficult to be effectively separated from aqueous solutions. Utilizing magnetism can solve this problem. Magnetic absorbents can conveniently facilitate the separation of materials from wastewater with use of a magnet [13–17]. Moreover, magnetic nanoparticles (Fe_3O_4) prepared by co-precipitation [18] are hydrophilic. Hence, we can add magnetic nanoparticles (Fe_3O_4) in the process of inverse suspension cross-linked method to obtain magnetic PVA microspheres.

Tetrazole, humic acid, 2-aminothiophenol, and other chemicals have been modified by the reaction of useful organic moieties. These methods could result in excellent adsorption performance [19–21]. Chelating materials, particularly chelating resins with nitrogen-containing or oxygen-containing complex ligands, such as amino, nitro carboxyl, and ethylenediamine, have been proven to chelate large amounts of heavy metal ions. Ethylenediamine tetra acetic acid (EDTA) has multiple lone pairs of electrons and can strongly attract heavy metal ions [22,23]. Therefore, synthesized ideal EDTA-type absorbents have emerged in, such as PS-EDTA resin [24].

Based on the above analysis, we attempted to prepare PVA microspheres with embedded magnetic nanoparticles (Fe_3O_4), and then functionalized with amino and EDTA groups, as illustrated in Fig. 1. The performance of the N-MPVA microspheres in the removal of toxic heavy metal ions was investigated. The resulting products were designed to adsorb different mono, di, and tri-valent heavy metal ions, particularly Ag^+, Cu^{2+}, and Cr^{3+}, from the aqueous solutions. This type of material exhibited excellent performance in terms of removal of heavy metal ions with different valences, and separation by an external magnetic field, from aqueous solutions. The structure, composition, and magnetic property of the N-MPVA microspheres were characterized with scanning electron microscopy (SEM), infrared spectroscopy (FTIR), X-ray photoelectron spectroscopy (XPS), and vibrating sample magnetometer (VSM).

2. Materials and methods

2.1. Materials

All reagents used in this study were of AR grade. PVA (1,750 ± 50), paraffin, Span-80, epichlorohydrin (EPC), ethanediamine, $AgNO_3$, $CuSO_4{\cdot}10H_2O$, and $Cr(NO_3)_3{\cdot}9H_2O$ were obtained from Sinopharm Chemical Reagent Co. Ltd (Beijing, China). Glutaraldehyde, tetrabutyl ammonium bromide (TBAB), and sodium chloroacetate were obtained from Sigma-Aldrich Reagent Company (Shanghai, China).

2.2. Preparation of the magnetic polyvinyl acetate microspheres

PVA (4 g) and Fe_3O_4 nanoparticles (0.4 g) which were prepared in advance by co-precipitation were dissolved in 40 mL distilled water with vigorous mechanical stirring in a boiling water bath for 1 h. After the mixture was cooled to room temperature, liquid paraffin (80 mL) and Span-80 (2 g) were added to the flask with continuous stirring at 60℃ for 2 h. Then, the temperature of boiling water was adjusted to 80℃. HCl (0.1 M, 2 mL) and glutaraldehyde (50%, 4 mL) were rapidly dropped under continuous stirring for 30 min. Finally, the magnetic PVA microspheres were rinsed repeatedly with petroleum ether to remove impurities and left to dry completely for few days.

2.3. Preparation of N-MPVA microspheres

Magnetic polyvinyl acetate (MPVA) (2 g), EPC (5 mL), and HCl (0.01 M, 100 mL) were mixed and heated in a water bath with mechanical stirring at 80℃ for 2 h. The products were then rinsed repeatedly with distilled water and left to dry completely for a few days. The resulting products, sodium hydroxide (2.5 g), ethanediamine (20 mL), and TBAB (0.1 g) were then mixed in 20 mL distilled water and heated in a water bath with continuous mechanical stirring at 85℃ for 6 h. The products were rinsed thoroughly with distilled water and ethanol to remove impurities and then left to dry completely for few days. The resulting products, sodium hydroxide (2.5 g), TBAB

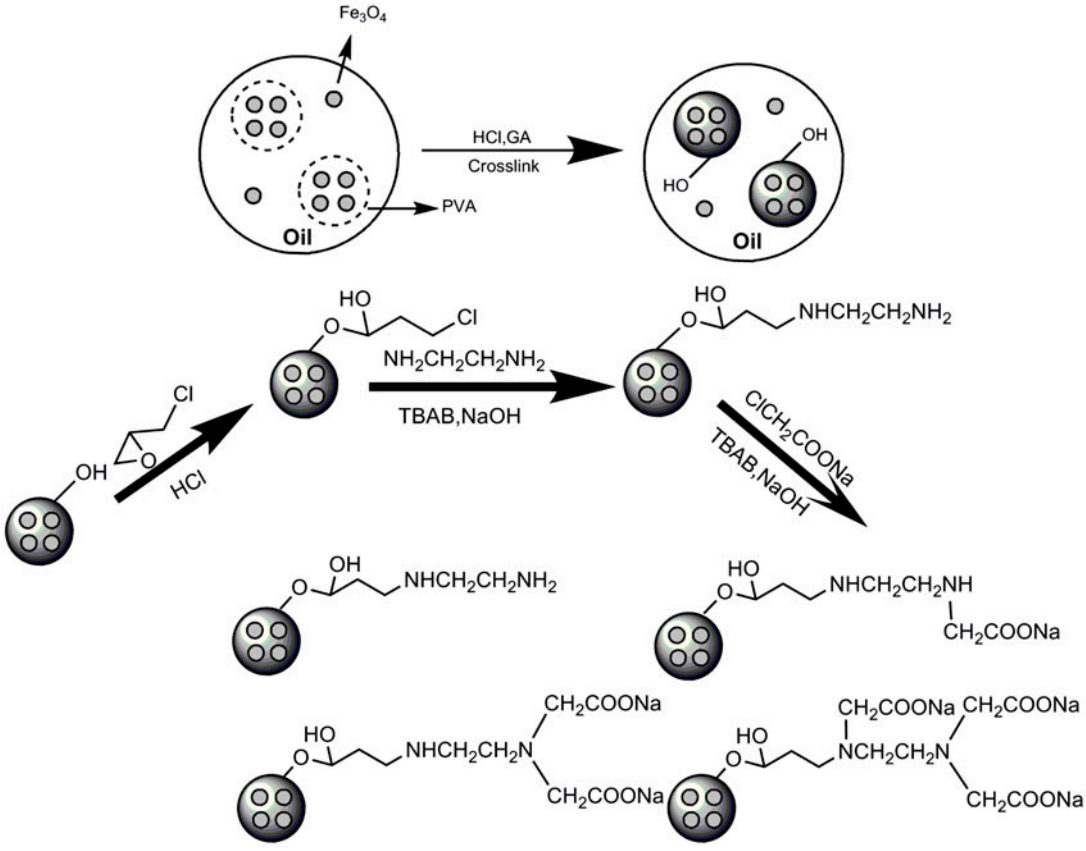

Fig. 1. Synthetic routes of N-MPVA microspheres.

(0.1 g), and sodium chloroacetate (2.52 g) were dissolved in 20 mL distilled water. The mixture was heated in a water bath with continuous mechanical stirring at 85°C for 6 h. The resulting products were rinsed repeatedly with distilled water and ethanol, and then left to dry completely for a few days.

2.4. Apparatus

The size and surface morphologies of the N-MPVA microspheres were visualized with a Hitachi S-4800 scanning electron microscope (Japan). The samples were sputter-coated with gold for 60 s and then visualized at an accelerating voltage of 5 kV. The infrared spectra of the N-MPVA microspheres were obtained by a TENSOR27 Perkin–Elmer FTIR spectrum (America). The resulting products were measured by ATR instrument. XPS was performed on the final N-MPVA microspheres with a PHI 5000 VersaProbe electron spectrometer (Japan). The magnetism of the resulting product was measured with a MPMS7 superconducting quantum interference device magnetometer (America). Zeta potentials were measured by a Nano–Z Zeta potential measurement analyzer (England). The concentrations of heavy metal ions in the aqueous solutions were analyzed with a Thermo 6300 ICP Spectrometer (America).

3. Adsorption experiments

To study the effect of different parameters, such as contact time, initial concentrations, solution pH, ionic competition, and reusability, we investigated the adsorption behavior of Ag^{+}, Cu^{2+}, and Cr^{3+} on N-MPVA. The data were used to calculate the amounts of heavy metal ions adsorbed Q (mg g^{-1}) with the use of Eq. (1):

$$Q = \frac{(C_i - C_e) \times V}{m} \quad (1)$$

where Q (mg g^{-1}) is the adsorption capacity of the magnetic absorbent; C_i and C_e (mg L^{-1}) are the initial and equilibrium concentrations of heavy metal ions, respectively; V (L) is the solution volume of heavy

metal ions; and m (g) is the mass of the N-MPVA microspheres.

3.1. Adsorption isotherm experiments

The adsorption isotherm batch experiments were performed as follows: N-MPVA (2 mg) was added to a heavy metal ion solution (Ag^+, Cu^{2+}, and Cr^{3+}, pH 5, 5 mL) by shaking at 180 rpm at 25°C for 6 h. The initial solutions of the heavy metal ions (Ag^+, Cu^{2+}, and Cr^{3+}) were varied from 10 to 100 mg L^{-1} and 150 mg L^{-1}. All pH values of the solutions were adjusted with HNO_3.

3.2. Adsorption kinetic experiments

The adsorption kinetic batch experiments were conducted as follows: N-MPVA (2 mg) was added to a heavy metal ion solution (Ag^+, Cu^{2+}, and Cr^{3+}, 100 mg L^{-1}, pH 5, 5 mL) with continuous shaking at 25°C at 180 rpm for 10, 20, 40 min, 1, 2, 4, 6, and 12 h. All pH values of the solutions were adjusted with HNO_3.

3.3. Different pH experiments

The surface electrical characteristic of N-MPVA in water was investigated through zeta potential measurement. The effects of solution pH were studied by addition of N-MPVA (2 mg) to the heavy metal ion solution (Ag^+, Cu^{2+}, and Cr^{3+}, 100 mg L^{-1}, 5 mL). The solution pH was varied from 2.0 to 12.0 by adding either HNO_3 or NaOH.

3.4. Ionic competition and reusability experiments

The desorption of heavy metal ions from N-MPVA was determined with 0.01 M HNO_3 as follows: magnetic absorbent (2 mg) was added into three heavy metal ion mixture solutions (Ag^+, Cu^{2+}, and Cr^{3+}, 100 mg L^{-1}, pH 5, 5 mL) after continuous shaking at 180 rpm at 25°C for 6 h, and the concentrations of the three heavy metal ions were measured. Heavy metal solutions were separated from the mixture with a magnet to recover the magnetic sample; the sample was dropped in HNO_3 (0.01 M, 10 mL) through shaking at 180 rpm for 2 h and left to dry for the next adsorption experiment. The adsorption–desorption cycles of N-MPVA during heavy metal removal were repeated three times with the same material. All pH values of the solutions were adjusted with HNO_3.

4. Results and discussion

4.1. Characterization of the N-MPVA microspheres

The surface morphology of the N-MPVA microspheres is shown in Fig. 2. The N-MPVA microspheres were approximately spherical in shape with a mean diameter of approximately 10 μm.

Fig. 3 shows the FTIR spectra of MPVA and N-MPVA. The initial vibration of O–H at 3,350 cm^{-1} was observed, and the band seen at 2,916 cm^{-1} was attributed to the vibration of C–H. Moreover, evident new peaks of N-MPVA appeared at 1,577 and 1,630 cm^{-1}, indicating the antisymmetric stretching vibration of amino and the stretching vibration of blue-shifted carboxyl because of connections with the polymer chain. The PVA microspheres had been modified successfully.

To illustrate the chemical characteristics well, the high-resolution spectra in XPS are shown in Fig. 4. The deconvolution of the C (1 s) spectra yielded eight main peaks: peak 1 (288.1 eV), –C=O; peak 2 (287.3 eV), –C–O; peak 3 (286.2 eV), –C–OH; peak 4 (285.7 eV), –C–N; peak 5 (285.2 eV), –C–NH_2; peak 6 (284.8 eV), C–H; peak 7 (284.5 eV), –C–H–; and peak 8 (284.1 eV), –C–C–. The N (1 s) spectra showed that the element N and its main forms exist as –C–N– (398.9 eV), –NH or –NH_2 (399.8 eV), and NH_4^+ (402 eV). The deconvolution of the O (1 s) spectra yielded four main peaks: peak 1 (532.5 eV), –C–O; peak 2 (531.9 eV), –OH; peak 3 (531.2 eV), –C=O; and peak 4 (530.3 eV), Fe_3O_4. These results illustrated that the PVA microspheres had been grafted with amino and EDTA groups, and a small amount of Fe_3O_4 was contained.

Fig. 5(a) shows the magnetic properties of N-MPVA determined on the basis of the magnetic

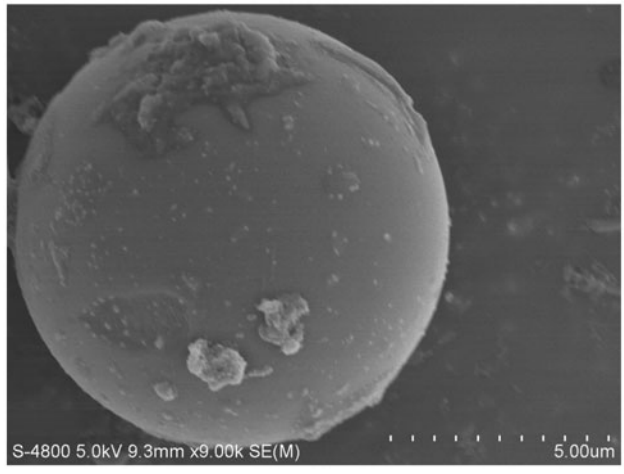

Fig. 2. SEM photograph of N-MPVA.

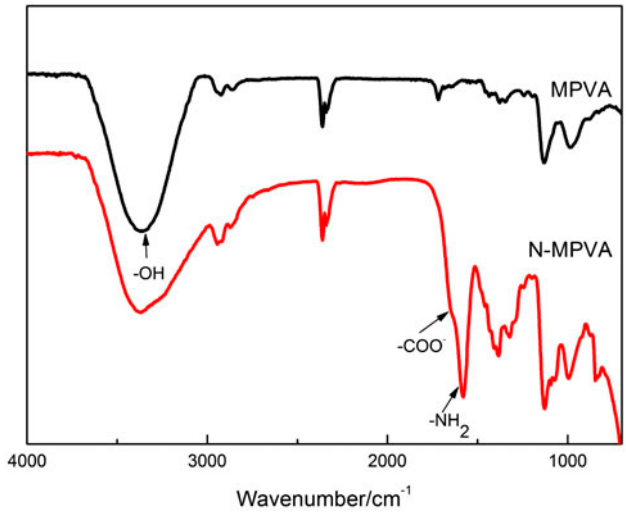

Fig. 3. FTIR spectra of MPVA and N-MPVA.

hysteretic curve measured at 25℃. The saturation magnetization value of N-MPVA was 4.89 emu g^{-1}. The simple attraction progress of the magnetic absorbent material by a magnet is described in Fig. 5(b). The dark brown magnetic materials were attracted to the container wall within 5 s after an external magnet was applied, which proved that N-MPVA could be used for magnetic separation.

4.2. Adsorption isotherm

To describe the adsorption isotherm well, the Langmuir and Freundlich isotherm models were used to illustrate isotherm performance. The Langmuir equation assumes that both adsorption and monolayer adsorption occur at specific homogeneous sites, and each site can accommodate only one molecule or atom [25–27]. The Langmuir isotherm is represented by the following expression:

$$\frac{1}{Q_e} = \frac{1}{Q_{max}} + \frac{1}{K_L Q_{max} C_e} \quad (2)$$

where Q_e is the equilibrium adsorption capacity (mg g^{-1}), C_e is the equilibrium concentration of heavy metal ions (mg L^{-1}), and K_L is the Langmuir isotherm parameter (L mg^{-1}).

The Freundlich isotherm is applied to non-ideal adsorption on heterogeneous surfaces, as well as to multi-layer adsorption [28,29]. The Freundlich isotherm is described as follows:

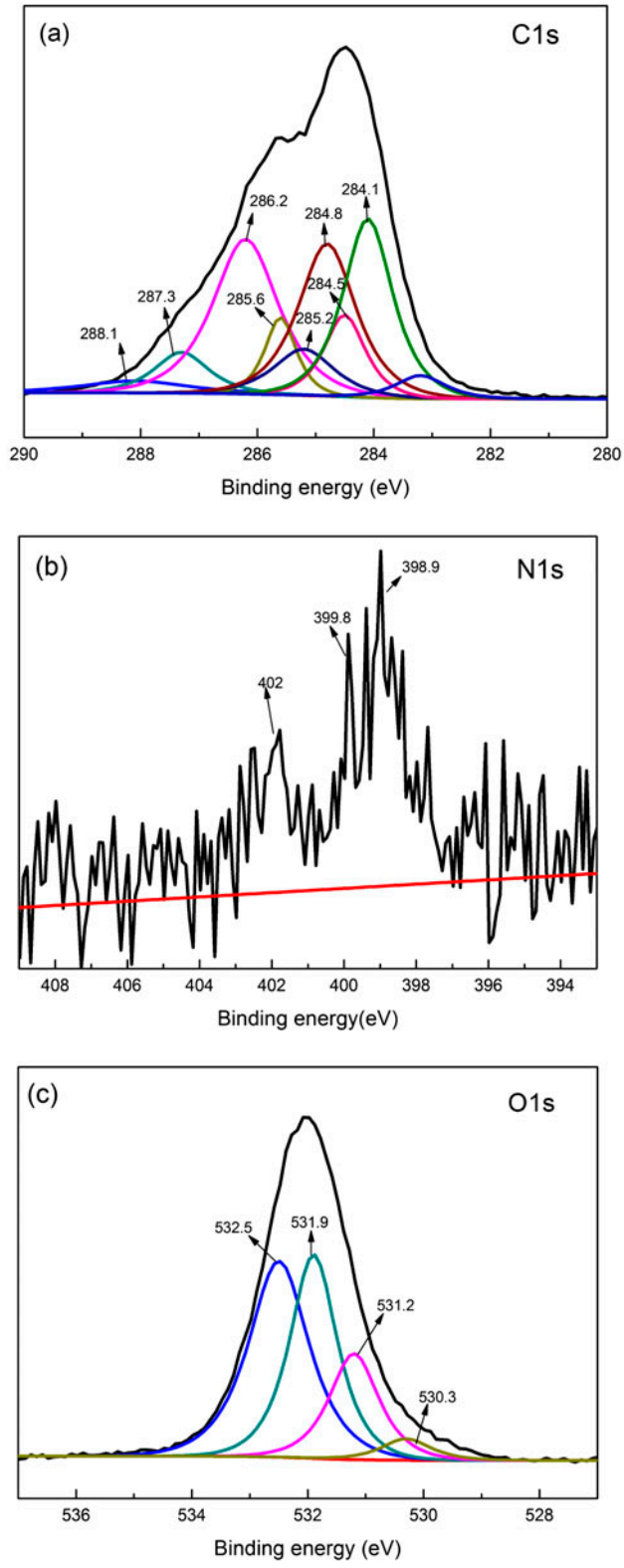

Fig. 4. X-ray photoelectron spectra of N-MPVA: (a) C (1 s) spectra, (b) N (1 s) spectra, and (c) O (1 s) spectra.

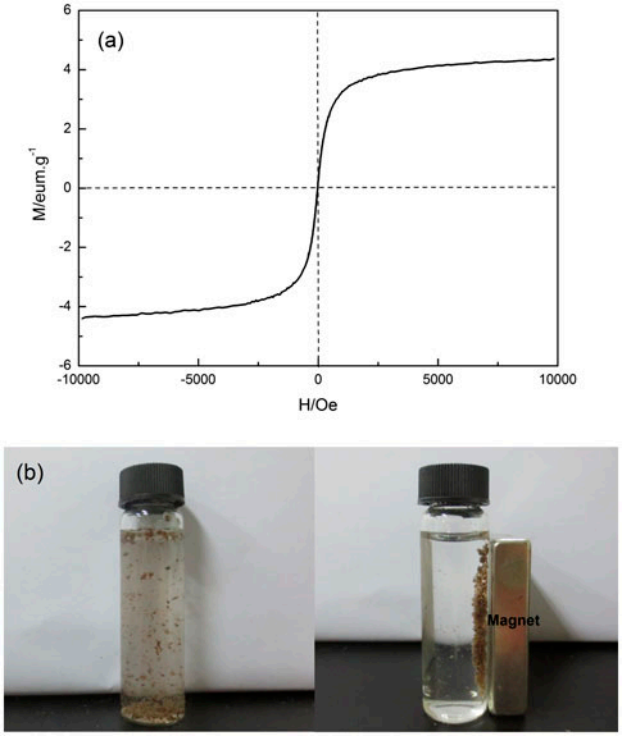

Fig. 5. (a) Magnetization curve of N-MPVA and (b) photographs of the magnetic separation progress of N-MPVA.

$$\log(Q_e) = \frac{1}{n \log C_e} + \log(K_F) \quad (3)$$

where Q_e is the equilibrium adsorption capacity (mg g^{-1}), C_e is the equilibrium concentration of heavy metal ions (mg L^{-1}), $1/n$ is the heterogeneity factor, and K_F is the Freundlich isotherm parameter [(L $(mg^{1-1/n}\, g)^{-1}$].

Fig. 6 displays the different adsorption isotherms on N-MPVA. The adsorption kinetic parameters for the adsorption of heavy metal ions (Ag^+, Cu^{2+}, and Cr^{3+}) by the magnetic absorbent are given in Table 1. K_L is determined from the slope and intercept of the linear plots of C_e/Q_e vs. C_e [Fig. 6(a)], and the values of K_F and $1/n$ are determined from the slope and intercept of the linear plot of $\ln Q_e$ vs. $\ln C_e$ [Fig. 6(b)]. Adsorption is generally favorable within $1 < n < 10$. In this study, all n values are within the above range for Ag^+, Cu^{2+}, and Cr^{3+}, and this result demonstrates that adsorption onto N-MPVA is favorable. The findings show that the correlation coefficient ($R^2 > 0.955$) of the Freundlich model is slightly higher than that of the Langmuir model ($R^2 > 0.945$), a result suggesting that multi-layer adsorption may fit well the adsorption. The N-MPVA microspheres not only have *Van der Waals* force and electrostatic effect, but also use hydroxy, amino, and EDTA groups to chelate heavy metal ions; so its adsorption for heavy metal ions is complex and comprehensive.

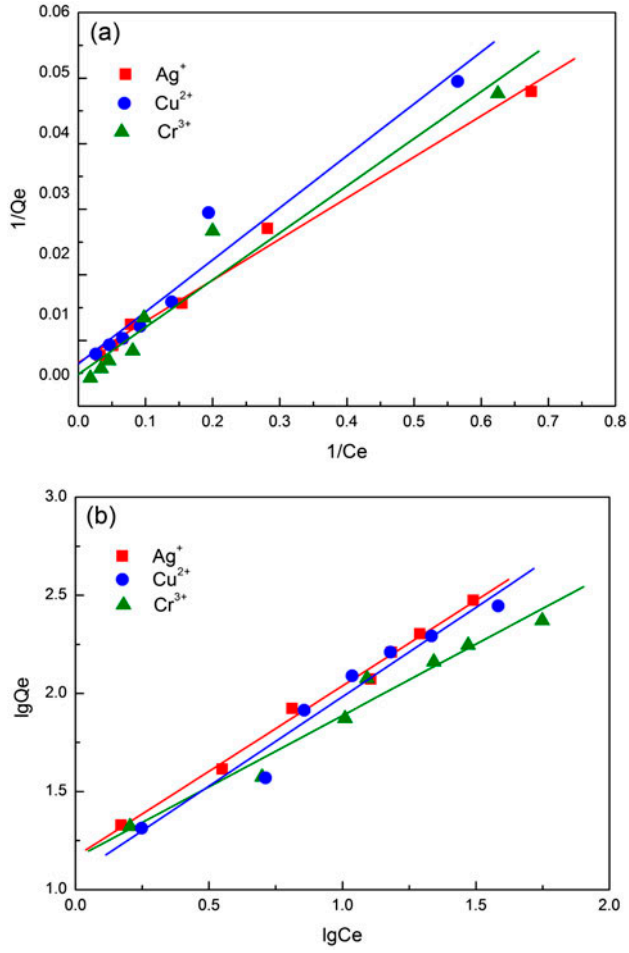

Fig. 6. (a) Langmuir adsorption isotherm of Ag^+, Cu^{2+}, and Cr^{3+} on N-MPVA and (b) Freundlich adsorption isotherm of Ag^+, Cu^{2+}, and Cr^{3+} on N-MPVA.

4.3. Adsorption kinetics

To investigate the adsorption mechanism of heavy metal ions (Ag^+, Cu^{2+}, and Cr^{3+}), pseudo-first-order and pseudo-second-order kinetic models are typically used to analyze the experimental data [30–32]. The equations of these two kinetic models are given in Eqs. (4) and (5):

$$\log(Q_e - Q_t) = \log(Q_e) - \frac{k_1 t}{2.303} \quad (4)$$

$$\frac{t}{Q_t} = \frac{1}{(k_2 Q_e^2)} + \frac{t}{Q_e} \quad (5)$$

Table 1
Langmuir and Freundlich isotherm constants for Ag^+, Cu^{2+}, and Cr^{3+} adsorption by N-MPVA

	Langmuir coefficient			Freundlich coefficient		
Absorbate	K_L (L mg^{-1})	Q_{max}(mg g^{-1})	R^2	K_F (L (mg$^{1-1/n}$) g^{-1})	$1/n$	R^2
Ag^+	0.0324	454.6	0.991	14.74	1.150	0.992
Cu^{2+}	0.0233	500.0	0.950	11.82	1.099	0.959
Cr^{3+}	0.0669	208.3	0.950	14.47	1.376	0.967

where Q_e is the equilibrium adsorption capacities (mg g^{-1}), Q_t is the adsorption capacities at time t, k_1 is the pseudo-first-order equilibrium rate parameter (min^{-1}), and k_2 is the pseudo-second-order rate parameter (g mg^{-1} min^{-1}).

The validity of the two models can be verified from the linear plots of log (Q_e−Q_t) vs. t and t/Q_t vs. t. The slopes and intercepts of each linear plot in Fig. 7 are used to calculate the adsorption rate constants (k_1 and k_2) and the amount of adsorption in equilibrium (Q_e). The adsorption kinetic parameters for the adsorption of heavy metal ions (Ag^+, Cu^{2+}, and Cr^{3+}) by the magnetic absorbent are shown in Table 2. We use the obtained correlation coefficient (R^2) to evaluate the applicability of both models and find that the experimental data fit the pseudo-second-order model ($R^2 > 0.980$) better than the pseudo-first-order model ($R^2 < 0.850$). This result indicates that the adsorbent systems can be well described by the former model.

The adsorption process can be evidently divided into three steps: an initial rapid step, a subsequent slow step, and a changeless step. The adsorption of heavy metal ions onto the absorbent is very rapid during the initial 10 min, during which the removal rate reaches up to 65.5, 63.0, and 71.0%, for Ag^+, Cu^{2+}, and Cr^{3+}, respectively. This rapid adsorption is attributed to physical and surface reactive adsorption because of a facilely immediate interaction between heavy metal ions and the active chelating groups on the surface of N-MPVA. Over the next 4 h, the removal rate only reaches up to 95.5, 77.8, and 79.0%, for Ag^+, Cu^{2+}, and Cr^{3+}, respectively, because of the reactive chelating reaction, a result suggesting the heavy metal ions start to diffuse onto the surface of microspheres, find the site of chelation, and prepare doing chelation. The heavy metal ions that adhered onto the surface of N-MPVA stop the rest of the heavy metal ions from approaching the microspheres, and this phenomenon significantly slows down to reach adsorption equilibrium. After 6 h, all adsorption capacities and removal rates are nearly unchanged. Therefore, the adsorption equilibrium times of the heavy metal ions with different valences are all nearly 6 h. Fig. 8 also shows that

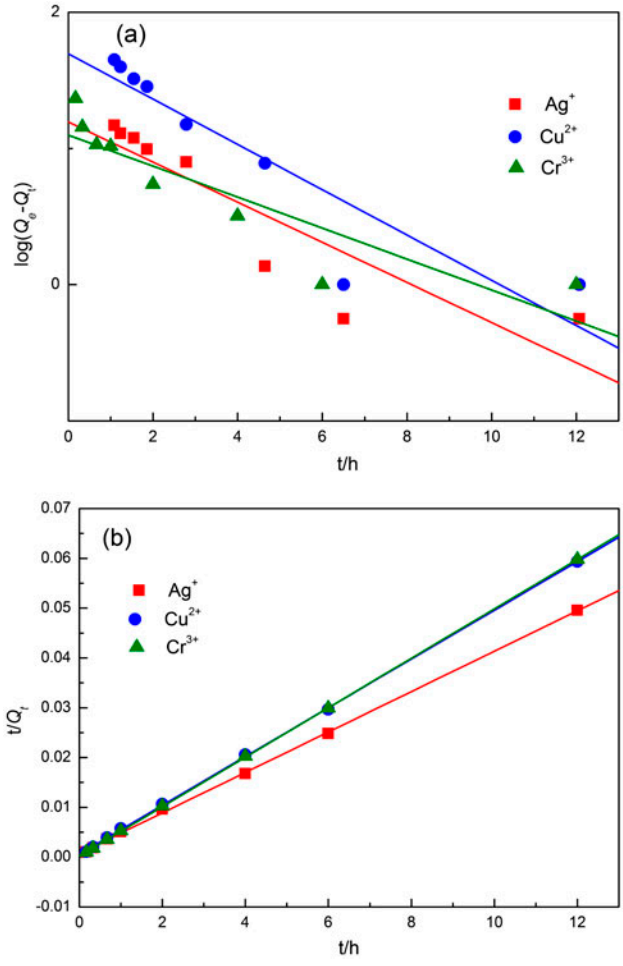

Fig. 7. (a) Pseudo-first-order model of Ag^+, Cu^{2+} and Cr^{3+} on N-MPVA and (b) Pseudo-second-order model of Ag^+, Cu^{2+}, and Cr^{3+} on N-MPVA.

the adsorption capacity of Ag^+ is the highest among all three heavy metal ions. The adsorption mechanisms for heavy metal ions with different valences will be discussed later.

4.4. Effect of pH

pH is important to the adsorption behavior of heavy metal ions. We investigated the resulting zeta

Table 2
Kinetic parameters in the pseudo-first-order and pseudo-second-order equations for Ag^{+}, Cu^{2+}, and Cr^{3+} adsorption by N-MPVA

	Pseudo-first-order equations		Pseudo-second-order equations	
Absorbate	k_1	R^2	k_2	R^2
Ag^{+}	0.420	0.798	0.021	0.999
Cu^{2+}	0.356	0.842	0.040	0.999
Cr^{3+}	0.261	0.800	0.019	0.998

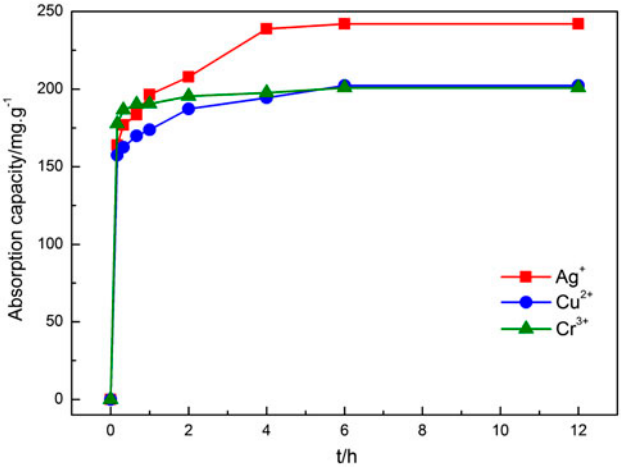

Fig. 8. Effect of different times of Ag^{+}, Cu^{2+}, and Cr^{3+} on N-MPVA.

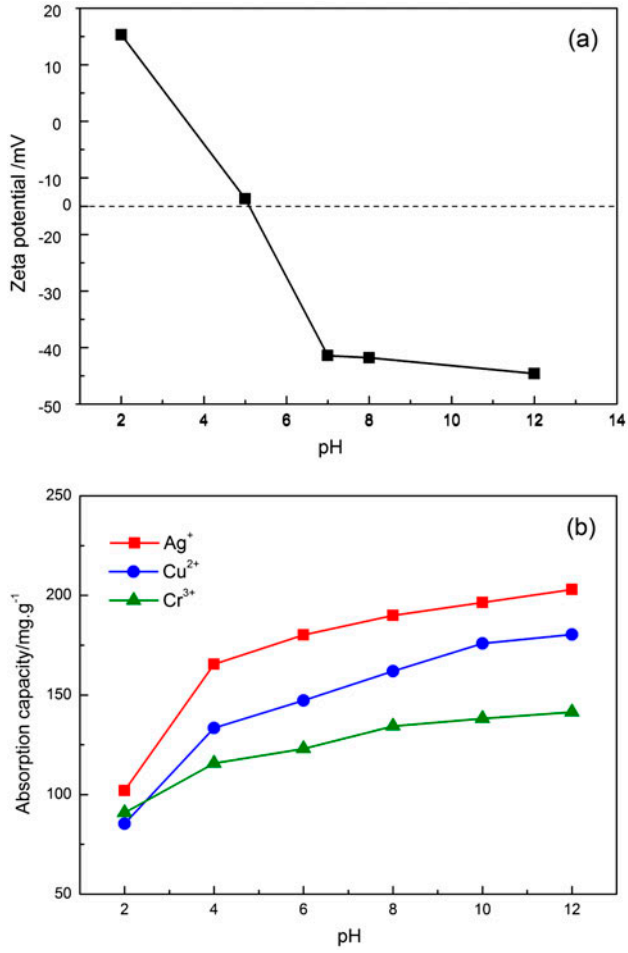

Fig. 9. (a) Zeta potentials of N-MPVA at pH values of 2, 5, 7, 8, and 12 and (b) influence of adsorption onto N-MPVA at pH values of 2, 4, 6, 8, 10, and 12.

potentials and effect of pH value on heavy metal ions (Ag^{+}, Cu^{2+}, and Cr^{3+}), as shown in Fig. 9(a). The isoelectric point (pI) of N-MPVA is close to 5. The electrostatic adsorption may influence the adsorption capacity. The zeta potential of N-MPVA gradually changes from positive at a low pH value (pH < 7), but it changes to negative at a high pH value (pH > 7). The effect of pH on the adsorption of heavy metal ions with different valences by N-MPVA can be seen in Fig. 9(b). The adsorption capacity increases with the solution pH (2–4), whereas an increase in the adsorption capacity slows down with the solution pH (4–6). The chelation mechanism is attributed to the less insignificant competitive adsorption of hydrogen ions. Chelating Cu^{2+} can be taken as an example, as expressed by Eqs. (6)–(9) [26,33]:

$$-NH_2 + H^+ \rightarrow -NH_3^+ \quad (6)$$

$$-NH_2 + Cu^{2+} \rightarrow -NH_2Cu^{2+} \quad (7)$$

$$-NH_2 + OH^- \rightarrow -NH_2OH^- \quad (8)$$

$$-NH_2OH^- + Cu^{2+}(\text{or}\,CuOH^+) \rightarrow -NH_2OH^- \cdots Cu^{2+}\,(\text{or} - NH_2OH^- \cdots CuOH^+) \quad (9)$$

At low solution pH (2–4), more $-NH_2$ were converted to $-NH_3^+$. Only few $-NH_2$ sites were available for heavy metal ion adsorption. Electrostatic repulsion also existed between the heavy metal ions and $-NH_3^+$. The reaction in Eq. (6) proceeded to the left with increasing pH values and induced an increase in the number of $-NH_2$ sites for heavy metal ions, suggesting that the adsorption capacity also increased, as indicated in Eq. (7). Both electrostatic repulsion and chelating adsorption resulted in a rapid increase in heavy

metal ion adsorption with the increase in pH values. While the pH > 4, the adsorption of heavy metal ions through electrostatic attraction might increase, as shown in Eqs. (8) and (9). The adsorption capacity of the microspheres gradually approached saturation.

4.5. Ionic competition and reusability

A magnetic absorbent will have different adsorption ability depending on heavy metal ions involved. Therefore, the ionic competition was investigated by the addition of three heavy metal ions with different valences into a flask. The adsorption capability for heavy metal ions with different valences is shown in Fig. 10. The adsorption dosage for heavy metal ions was in the order of Ag^{+} (135.0 mg g^{-1}) > Cu^{2+} (48.5 mg g^{-1}) > Cr^{3+} (33.0 mg g^{-1}). Adsorption capability decreased with the valence of the heavy metal ions. N-MPVA microsphere used $-NH_2$ or EDTA groups to chelate the heavy metal ions. There similarly existed a 1:1 M-EDTA chelate (M represented Ag^{+}, Cu^{2+}, and Cr^{3+}). However, differently, Ag^{+} may need only 2 $-NH_2$ to form $Ag[NH_3]_2^+$, Cu^{2+} may need 4 $-NH_2$ to be comparable with $Cu[NH_3]_4^+$, and Cr^{3+} may need 6 $-NH_2$ to be comparable with $Cr[NH_3]_6^+$, as explained in Table 3. Furthermore, stereospecific blockade was found in the process of chelation, and the difficulty in chelating heavy metal ions was in the order of Ag^{+} < Cu^{2+} < Cr^{3+}. The number of groups adsorbing Ag^{+} was highest, and the number of groups adsorbing Cr^{3+} was smallest.

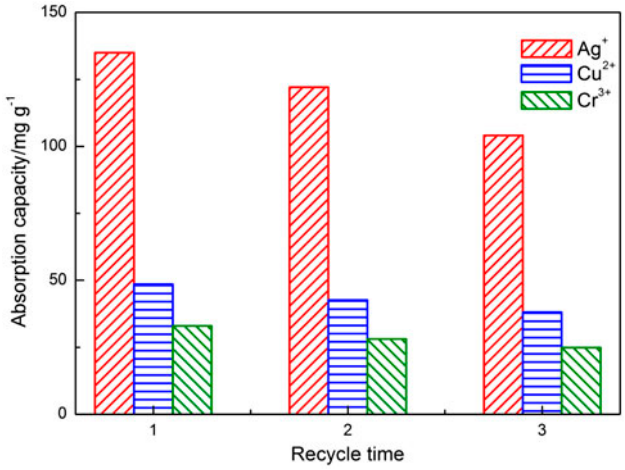

Fig. 10. Ionic competition and reusability of Ag^{+}, Cu^{2+}, and Cr^{3+} onto N-MPVA.

Through the desorption experiment, we also proved the excellent repeated availability of N-MPVA

Table 3
Chelating mechanism of heavy metal ions with different valences onto N-MPVA

	Amino groups	EDTA groups (M represents different heavy metal ions)
Ag^{+}	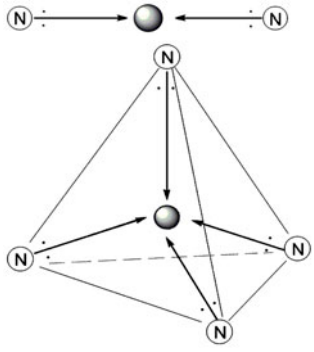	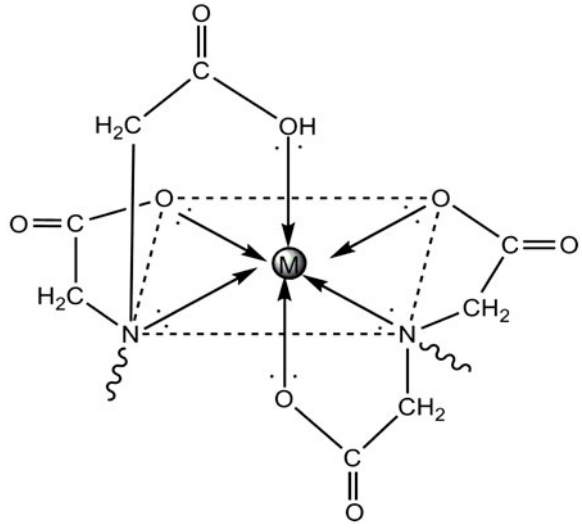
Cu^{2+}		
Cr^{3+}	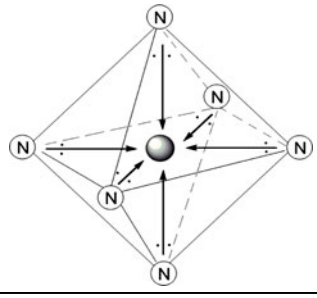	

for heavy metal ion removal. After the adsorption equilibrium was reached, N-MPVA was separated from the aqueous solutions with a magnet. Thereafter, 0.01 M HNO_3 was mixed with the absorbent to release the heavy metal ions. After regenerating for three times, the adsorption capacities of heavy metal ions with different valences onto N-MPVA are as shown in Fig. 10. The loss of adsorption capacity of N-MPVA did not exceed 25% after three recycles.

5. Conclusions

In this study, the preparation and adsorption performance of N-MPVA was investigated for the removal of different mono-, di-, and tri- valent heavy metals from aqueous systems. The synthetic condition of N-MPVA is moderate, and the maximum temperature is below 100˚C. SEM showed that synthetic N-MPVA had an approximate spherical shape, and its saturation magnetization value was 4.89 $emu \cdot g^{-1}$ via VSM. FTIR and XPS illustrated that the synthetic product had a chemical structure similar to EDTA, as well as a large amount of $–NH_2$, which possibly contributed to the chelation of heavy metal ions. The synthetic absorbent was used to remove Ag^+, Cu^{2+}, and Cr^{3+} from aqueous systems through the amino and EDTA groups chelation. Adsorption isotherm and adsorption kinetic suggested its adsorption for heavy metal ions was complex and comprehensive. Desorption experiments demonstrated that the loss of adsorption capacity did not exceed 25% after three recycles. With its high adsorption capacity, separation convenience, and environmental soundness, N-MPVA is a promising alternative for heavy metal ions removal and recovery from wastewater.

Acknowledgments

We are grateful for grants from National Natural Science Foundation of China (grant number 51308183), Natural Science Foundation of Jiangsu Province of China (grant number BK20130828), National Key Technologies R&D Program of China (2012BAB03B04), and Major Science and Technology Program for Water Pollution Control and Treatment (2012ZX07103-005).

References

[1] S.E. Bailey, T.J. Olin, R.M. Bricka, D.D. Adrian, A review of potentially low-cost sorbents for heavy metals, Water Res. 33 (1999) 2469–2479.
[2] M. Malandrino, O. Abollino, A. Giacomino, M. Aceto, E. Mentasti, Adsorption of heavy metals on vermiculite: Influence of pH and organic ligands, J. Colloid Interface Sci. 299 (2006) 537–546.
[3] C. Marambio-Jones, E.M.V. Hoek, A review of the antibacterial effects of silver nanomaterials and potential implications for human health and the environment, J. Nanopart. Res. 12 (2010) 1531–1551.
[4] S. Meier, R. Azcón, P. Cartes, F. Borie, P. Cornejo, Alleviation of Cu toxicity in *Oenothera picensis* by copper-adapted arbuscular mycorrhizal fungi and treated agrowaste residue, Appl. Soil Ecol. 48 (2011) 117–124.
[5] M. Jain, V.K. Garg, K. Kadirvelu, Chromium(VI) removal from aqueous system using *Helianthus annuus* (sunflower) stem waste, J. Hazard. Mater. 162 (2009) 365–372.
[6] T.A. Davis, B. Volesky, A. Mucci, A review of the biochemistry of heavy metal biosorption by brown algae, Water Res. 37 (2003) 4311–4330.
[7] V.N. Tirtom, A. Dinçer, S. Becerik, T. Aydemir, A. Çelik, Removal of lead (II) ions from aqueous solution by using crosslinked chitosan-clay beads, Desalin. Water Treat. 39 (2012) 76–82.
[8] C.L. Massocatto, E.C. Paschoal, N. Buzinaro, T.F. Oliveria, C.R.T. Tarley, J. Caetano, A.C. Gonçalves, D.C. Dragunski, K.M. Diniz, Preparation and evaluation of kinetics and thermodynamics studies of lead adsorption onto chemically modified banana peels, Desalin. Water Treat. 51 (2013) 5682–5691.
[9] A. Fouladi Tajar, T. Kaghazchi, M. Soleimani, Adsorption of cadmium from aqueous solutions on sulfurized activated carbon prepared from nut shells, J. Hazard. Mater. 165 (2009) 1159–1164.
[10] L.C.A. Oliveira, D.I. Petkowicz, A. Smaniotto, S.B.C. Pergher, Magnetic zeolites: A new adsorbent for removal of metallic contaminants from water, Water Res. 38 (2004) 3699–3704.
[11] Y. Liu, X. Sun, B. Li, Adsorption of Hg^{2+} and Cd^{2+} by ethylenediamine modified peanut shells, Carbohydr. Polym. 81 (2010) 335–339.
[12] X. Bai, Z.F. Ye, Y.Z. Qu, Y.F. Li, Z.Y. Wang, Immobilization of nanoscale Fe0 in and on PVA microspheres for nitrobenzene reduction, J. Hazard. Mater. 172 (2009) 1357–1364.
[13] Z. Wang, D. Wu, G. Wu, N. Yang, A. Wu, Modifying Fe_3O_4 microspheres with rhodamine hydrazide for selective detection and removal of Hg^{2+} ion in water, J. Hazard. Mater. 244–245 (2013) 621–627.
[14] S. Tao, C. Wang, W. Ma, S. Wu, C. Meng, Designed multifunctionalized magnetic mesoporous microsphere for sequential sorption of organic and inorganic pollutants, Microporous Mesoporous Mater. 147 (2012) 295–301.
[15] M. Monier, D.M. Ayad, D.A. Abdel-Latif, Adsorption of Cu(II), Cd(II) and Ni(II) ions by cross-linked magnetic chitosan-2-aminopyridine glyoxal Schiff's base, Colloids Surf., B 94 (2012) 250–258.
[16] J.L. Gong, X.Y. Wang, G.M. Zeng, L. Chen, J.H. Deng, X.R. Zhang, Q.Y. Niu, Copper (II) removal by pectin–iron oxide magnetic nanocomposite adsorbent, Chem. Eng. J. 185–186 (2012) 100–107.
[17] A.Z.M. Badruddoza, Z.B.Z. Shawon, T.W.J. Daniel, K. Hidajat, M.S. Uddin, Fe_3O_4 cyclodextrin polymer nanocomposites for selective heavy metals removal from industrial wastewater, Carbohydr. Polym. (2012) 322–332.

[18] A.H. Lu, E.L. Salabas, F. Schüth, Magnetic nanoparticles: Synthesis, protection, functionalization, and application, Angew. Chem. Int. Ed. 46 (2007) 1222–1244.
[19] S. Yan, M. Zhao, G. Lei, Y. Wei, Novel tetrazole-functionalized absorbent from polyacrylonitrile fiber for heavy-metal ion adsorption, J. Appl. Polym. Sci. 125 (2012) 382–389.
[20] P. Stathi, Y. Deligiannakis, Humic acid-inspired hybrid materials as heavy metal absorbents, J. Colloid Interface Sci. 351 (2010) 239–247.
[21] V. Lemos, P. Baliza, Amberlite XAD-2 functionalized with 2-aminothiophenol as a new sorbent for on-line preconcentration of cadmium and copper, Talanta 67 (2005) 564–570.
[22] M.C. Diez, D. Pouleurs, R. Navia, G. Vidal, Effect of EDTA and Fe-EDTA complex concentration on TCF Kraft mill effluent degradability. Batch and continuous treatments, Water Res. 39 (2005) 3239–3246.
[23] O.K. Júnior, L.V.A. Gurgel, R.P. de Freitas, L.F. Gil, Adsorption of Cu(II), Cd(II), and Pb(II) from aqueous single metal solutions by mercerized cellulose and mercerized sugarcane bagasse chemically modified with EDTA dianhydride (EDTAD), Carbohydr. Polym. 77 (2009) 643–650.
[24] L. Yang, Y. Li, L. Wang, Y. Zhang, X. Ma, Z. Ye, Preparation and adsorption performance of a novel bipolar PS-EDTA resin in aqueous phase, J. Hazard. Mater. 180 (2010) 98–105.
[25] R. Naseem, S. Tahir, Removal of Pb(II) from aqueous/acidic solutions by using bentonite as an adsorbent, Water Res. 35 (2001) 3982–3986.
[26] M. Dakiky, M. Khamis, A. Manassra, M. Mer'eb, Selective adsorption of chromium(VI) in industrial wastewater using low-cost abundantly available adsorbents, Adv. Environ. Res. 6 (2002) 533–540
[27] A.A.A. Emara, M.A. Tawab, M.A. El-ghamry, M.Z. Elsabee, Metal uptake by chitosan derivatives and structure studies of the polymer metal complexes, Carbohydr. Polym. 83 (2011) 192–202.
[28] F. Rivas, F. Beltran, O. Gimeno, J. Frades, F. Carvalho, Adsorption of landfill leachates onto activated carbon. Equilibrium and kinetics, J. Hazard. Mater. 131 (2006) 170–178.
[29] I. Kavianinia, P.G. Plieger, N.G. Kandile, D.R.K. Harding, New hydrogels based on symmetrical aromatic anhydrides: Synthesis, characterization and metal ion adsorption evaluation, Carbohydr. Polym. 87 (2012) 881–893.
[30] S. Azizian, Kinetic models of sorption: A theoretical analysis, J. Colloid Interface Sci. 276 (2004) 47–52.
[31] Y.S. Ho, G. McKay, Pseudo-second order model for sorption processes, Process Biochem. 34 (1999) 451–465.
[32] V.B.H. Dang, H.D. Doan, T. Dang Vu, A. Lohi, Equilibrium and kinetics of biosorption of cadmium(II) and copper(II) ions by wheat straw, Bioresour. Technol. 100 (2009) 211–219.
[33] S.H. Huang, D.H. Chen, Rapid removal of heavy metal cations and anions from aqueous solutions by an amino-functionalized magnetic nano-adsorbent, J. Hazard. Mater. 163 (2009) 174–179.